Title

Consequences of Exposure to Light at Night on the Pancreatic Islet Circadian Clock and Function in Rats

Journal

Diabetes, 62(10)

ISSN

0012-1797

Authors

Qian, Jingyi
Block, Gene D
Colwell, Christopher S
et al.

Publication Date

2013-10-01

DOI

10.2337/db12-1543

Peer reviewed

Consequences of Exposure to Light at Night on the Pancreatic Islet Circadian Clock and Function in Rats

Jingyi Qian,[1,2] Gene D. Block,[2] Christopher S. Colwell,[2] and Aleksey V. Matveyenko[1]

There is a correlation between circadian disruption, type 2 diabetes mellitus (T2DM), and islet failure. However, the mechanisms underlying this association are largely unknown. Pancreatic islets express self-sustained circadian clocks essential for proper β-cell function and survival. We hypothesized that exposure to environmental conditions associated with disruption of circadian rhythms and susceptibility to T2DM in humans disrupts islet clock and β-cell function. To address this hypothesis, we validated the use of *Per-1*:LUC transgenic rats for continuous longitudinal assessment of islet circadian clock function ex vivo. Using this methodology, we subsequently examined effects of the continuous exposure to light at night (LL) on islet circadian clock and insulin secretion in vitro in rat islets. Our data show that changes in the light–dark cycle in vivo entrain the phase of islet clock transcriptional oscillations, whereas prolonged exposure (10 weeks) to LL disrupts islet circadian clock function through impairment in the amplitude, phase, and interislet synchrony of clock transcriptional oscillations. We also report that exposure to LL leads to diminished glucose-stimulated insulin secretion due to a decrease in insulin secretory pulse mass. Our studies identify potential mechanisms by which disturbances in circadian rhythms common to modern life can predispose to islet failure in T2DM. ***Diabetes*** **62:3469–3478, 2013**

Type 2 diabetes mellitus (T2DM) is characterized by islet failure due to loss of β-cell function and mass (1,2). The cause of islet failure in T2DM involves an interaction among genetic predisposition and confounding environmental factors (3). In recent years, environmental conditions associated with disruption of circadian rhythms (e.g., rotating shift work, light during the night, sleep loss, etc.) have become prevalent and have been reported to augment susceptibility to T2DM (4,5). Importantly, the correlation between circadian disruption and T2DM is partly attributed to loss of β-cell function and mass (6–8). Despite a strong association among circadian disruption, T2DM, and islet failure, the mechanisms underlying this link remain under investigation.

Circadian rhythms allow organisms to align internal metabolism as well as physiological and behavioral attributes to changes in the light–dark (LD) cycle. The "central clock" of the circadian system in mammals is localized in the suprachiasmatic nucleus (SCN) of the hypothalamus. The SCN consists of molecular oscillators (clocks), operating within individual neurons, governed by precise transcriptional-translational feedback loops (9). Moreover, molecular oscillators are also present in tissues outside of the SCN, including pancreatic islets (10). The SCN functions to synchronize peripheral clocks to the LD cycle via a combination of neuronal, behavioral, and endocrine outputs (11). The mechanism driving the molecular clocks is governed by a set of core "clock genes." In short, *CLOCK* and *BMAL1* are two helix-loop-helix transcription factors that are essential components of the core circadian clock (12), and when dimerized, activate transcription of the *Period* (PER) genes and *Cryptochrome* (CRY) genes through a circadian E-box regulatory element. Once translated, PER and CRY translocate to the nucleus where they function as negative regulators of their own transcription by interacting with the CLOCK/BMAL1 complex, thereby completing the negative feedback loop (13). This complex oscillatory network sustains 24-h transcriptional oscillations and, importantly, synchronizes transcription of clock effector genes to changes in the LD cycle (14).

Studies suggest that β-cell secretory function and survival is under transcriptional control of the circadian clock. β-Cell secretory capacity shows a circadian pattern, which is impaired upon exposure to aberrant LD cycles or SCN lesions (15–17). Circadian disruption in diabetes-prone rodents accelerates hyperglycemia through induction of islet failure (8). Moreover, clock gene mutants are hyperglycemic, glucose-intolerant, and lack appropriate insulin secretion (10,18,19). However, despite increased insights into the role of the circadian system in islet function, little data are available on the effects of environmental conditions associated with circadian disruption, common to modern life, on the integrity of the islet circadian clock and function. Consequently, to address this issue, we *1*) validated the use of transgenic rats in which the *Per-1* promoter was linked to a luciferase reporter (*Per-1*:LUC) for longitudinal assessment of islet circadian clock function ex vivo, *2*) tested the hypothesis that changes in the LD cycle in vivo entrain the phase of islet clock transcriptional oscillations, and *3*) tested the hypothesis that exposure to environmental conditions associated with circadian disruption (i.e., continuous exposure to light at night), disrupts islet circadian clock and function.

RESEARCH DESIGN AND METHODS

Animal husbandry and behavioral monitoring. The study used 43 wild-type (WT) and 37 transgenic rats in which the mouse *Period-1* promoter was linked to luciferase reporter (*Per-1*:LUC) rats. The generation and validation of *Per-1*:LUC rats has been previously described (20). Rats were housed individually at the University of California, Los Angeles (UCLA), animal facility and kept in

From the [1]Larry L. Hillblom Islet Research Center, Department of Medicine, Division of Endocrinology, University of California, Los Angeles, David Geffen School of Medicine, Los Angeles, California; and the [2]Laboratory for Circadian and Sleep Medicine, Departments of Psychiatry and Biobehavioral Sciences, University of California, Los Angeles, David Geffen School of Medicine, Los Angeles, California.

Corresponding author: Aleksey V. Matveyenko, amatveyenko@mednet.ucla.edu.

Received 6 November 2012 and accepted 11 June 2013.

DOI: 10.2337/db12-1543

This article contains Supplementary Data online at http://diabetes.diabetesjournals.org/lookup/suppl/doi:10.2337/db12-1543/-/DC1.

environmentally controlled soundproof chambers under the standard 12/12-h LD cycle (lights on at 0600 h, lights off 1800 h, all times in Pacific Standard Time). Cages were outfitted with the optical beam sensor system to monitor circadian behavioral rhythms in activity and feeding (Respironics, Murrysville, PA). The UCLA Institutional Animal Care and Use Committee approved all experimental procedures.

Elucidation of behavioral, metabolic, and molecular circadian rhythms in WT rats under LD cycle. To establish diurnal behavioral, metabolic, and temporal profiles in circadian clock gene and protein expression in vivo, we used 2-month-old WT rats. Rats were kept in the standard LD cycle for 10 weeks, and behavioral rhythms in feeding and activity were monitored. Rats were subsequently euthanized every 4 h (n = 4–5 per time point; at 0200, 0600, 1000, 1400, 1800, and 2200 h). Blood was immediately collected and the pancreas quickly excised, with one part preserved for immunohistochemical analysis and another for laser microdissection of islets for in vivo clock gene expression assessment by real-time PCR.

Laser microdissection of islets for assessment of profiles in islet clock gene expression in WT rats under LD cycle. After euthanasia, the pancreas was harvested and embedded into optimal cutting temperature solution (Tissue-Tek, Torrance, CA), frozen on dry ice, and stored. Subsequently, complete longitudinal sections (8 μm) of pancreas were obtained using a precooled (−20°C) cryotome and mounted on ultraviolet irradiated nucleic acid-free polyethylene naphthalate membrane slides (Leica, Wetzlar, Germany). Slides were then immediately stained with hematoxylin to identify islets and subsequently laser microdissected (Leica LMD7000) with ~100 islets per time point per rat. Total islet RNA was isolated using Arcturus PicoPure extraction method (Applied Biosystems, Foster City, CA) and cDNA synthesis performed using the SuperScript III First-Strand synthesis kit (Invitrogen, Carlsbad, CA). The real-time PCR was performed with validated gene-specific primers for core clock genes (*Bmal-1* and *Per-1*) according to the manufacturer's instructions (7900HT Applied Biosystems).

Immunofluorescent staining for assessment of profiles in β-cell clock protein expression in WT rats under LD cycle. After euthanasia, the pancreas was immediately harvested and fixed in 4% paraformaldehyde. Paraffin-embedded pancreatic sections were costained by immunofluorescence for markers of islet endocrine cell types insulin (18-0067; Invitrogen), glucagon (G2654, Sigma-Aldrich, St. Louis, MO), pancreatic polypeptide (NB100-1793, Novus Biologicals, Littleton, CO), somatostatin (MAB354, Millipore, Billerica, MA), and core clock proteins BMAL-1 (sc-8550), PER-1 (sc-25362), and PER-2 (sc-25363) obtained from Santa Cruz Biotechnology. Slides were viewed using a Leica DM6000 microscope (Leica Microsystems, Bannockburn, IL) and images acquired using OpenLab 5 (PerkinElmer, Waltham, MA).

Longitudinal assessment of rat islet circadian clock ex vivo using islets isolated from *Per-1*:LUC rats. After euthanasia, rat islets were isolated from 2-month-old *Per-1*:LUC rats using standard collagenase method (performed always at 0900 Pacific Standard Time). Batches of 50 islets matched by size and diameter (using an ocular measuring device) were placed on PTFE membranes (Millipore) in culture dishes containing culture medium (serum-free, no sodium bicarbonate, no phenol red, Dulbecco's modified Eagle's medium [D50300-10L, Sigma-Aldrich] supplemented with 10 mmol/L HEPES [pH 7.2], 2 mmol/L glutamine, B27 [2%, GIBCO], and 0.1 mmol/L luciferin). To test glucose sensitivity of the islet clock (Fig. 2), culture medium was supplemented with 2, 5, 11, or 25 mmol/L D-glucose. For all subsequent studies (Figs. 3–6), islets were cultured in standard 11 mmol/L glucose rodent medium. Culture dishes containing islets were immediately placed into a LumiCycle luminometer (Actimetrics, Wilmette, IL) inside a light-resistant 37°C chamber with bioluminescence recorder photomultiplier tube detector. The bioluminescence signal was counted in 1-min bins every 10 min for at least 5 days, and data were normalized by subtraction of the 24-h running average from the raw data and then smoothed with a 2-h running average (Lumicycle Data Analysis, Actimetrics) (Supplementary Fig. 2). The peak was calculated as the highest point of smoothed data, and the free-running period was computed as the mean between the peaks in each cycle. The amplitude was summed by the highest point and the lowest point of the each cycle (21). *Per-1*–driven luciferase rhythms emanating from individual islets were imaged using an XR/MEGA-10Z cooled intensified charge-coupled device camera (Stanford Photonics, Inc., Palo Alto, CA). Isolated islets were cultured as previously described. Photon counts were integrated over 3 min with Piper control (Stanford Photonics) and processed with Image-J software (National Institutes of Health, Bethesda, MD). Amplitude, period, and the phase of Per-driven luciferase rhythms emanating from individual islets were calculated using Lumicycle Analysis software (Actimetrics). Phase coherence of islets was determined using Rayleigh plots, which were constructed by El-Temps software (Antoni Díez-Noguera, University of Barcelona, Barcelona, Spain).

Entrainment of the islet circadian clock by changes in the LD cycle. To test whether changes in the LD cycle in vivo entrain the phase of islet clock transcriptional oscillations, we studied *Per-1*:LUC rats acclimatized for 2 weeks to the standard 12/12-h LD cycle. Behavioral recording was performed as described to confirm robust circadian behavioral rhythms. Subsequently, we inverted the phase of the LD cycle by 12 h to DL (lights on at 1800 h, lights off at 0600 h) for 4 weeks and confirmed entrainment to the new DL cycle using behavioral recordings. At the end of the 4-week period, DL rats were euthanized, islets isolated, and the amplitude, phase, and period of islet-specific *Per*-driven luciferase rhythms was determined as described.

Effects of circadian disruption due to light at night on behavioral, metabolic, and molecular circadian rhythms in WT rats. Two-month-old WT rats were kept under lights on at night (LL) for 10 weeks, and induction of circadian arrhythmicity was confirmed by diurnal feeding and activity recordings. Subsequently, rats were euthanized every 4 h (n = 4–5 per time point; at 0200, 0600, 1000, 1400, 1800, and 2200 h) across the 24-h day, and blood and the pancreas were immediately collected for subsequent metabolic analysis.

We tested the hypothesis that chronic exposure to LL results in disruption of the islet clock function by studying nine *Per-1*:LUC rats. All rats were first acclimatized for 2 weeks to the standard LD cycle and then exposed to 10 weeks of the control LD cycle (n = 5) or 24-h LL (n = 4). Behavioral rhythms were monitored at baseline and during the study to confirm disruption of circadian rhythms in the LL rats. At the end of the 10-week experimental period, all LD and LL rats were euthanized, islets were isolated, and *Per-1*–driven bioluminescence rhythms were used to assess the amplitude, period, and the phase of the islet circadian clock, in batches of 50 islets (Fig. 4) and in individual islets (Fig. 5).

Islet isolations and assessment of β-cell function in vitro. Pancreatic islets were isolated using standard collagenase procedure. To assess the dose-dependent glucose responsiveness, batches of 20 islets were statically incubated in RPMI solution supplemented with 4, 8, 12, and 16 mmol/L glucose for 30 min at each glucose concentration. Different batches of 20 islets were also stimulated with 10 nmol/L exendin-4 or 250 μmol/L tolbutamide for 30 min for assessment of non–glucose-dependent insulin release. Supernatant and lysed islets were assayed by insulin ELISA. To assess the pulsatile mode of insulin secretion, islet perifusion experiments were performed (ACUSYST-S, Cellex Biosciences, Inc., Minneapolis, MN) (22). Batches of 20 islets were first exposed to 40 min of 4 mmol/L glucose in Krebs-Ringer bicarbonate buffer supplemented with 0.2% serum albumin, preheated to 37°C, and oxygenized with 95% O_2 and 5% CO_2, followed by 40 min of hyperglycemic perfusate (16 mmol/L glucose). Effluent was collected in 1-min intervals and assayed for insulin by ELISA for subsequent determination of total insulin secretory rate, insulin pulse mass, and insulin pulse interval (22).

Analytical procedures. Plasma glucose was measured by the glucose oxidase method (YSI Glucose Analyzer, Yellow Springs, OH). Insulin and C-peptide were measured using an ELISA assay (Alpco, Salem NH).

Statistical analysis and calculations. Activity and feeding recordings were analyzed using ClockLab software (Actimetrics). Circadian rhythms in β-cell function and insulin sensitivity were calculated using homeostasis model assessment indices (HOMA) of insulin sensitivity ($HOMA_{IR}$ = [glucose] × [insulin]/405; insulin in mU/L and glucose in mg/dL) and β-cell function ($HOMA_{\beta}$ = [20 × insulin]/[glucose − 3.5]; insulin in mU/L and glucose in mmol/L) (23). Statistical analysis was performed using ANOVA with the Fisher post hoc test where appropriate (Statistica; Statsoft, Tulsa, OK). Data in graphs are presented as means ± SEM and assumed statistically significant at $P < 0.05$.

RESULTS

Rats exhibit robust behavioral, metabolic, and molecular circadian rhythms under the LD cycle. Noninvasive monitoring of locomotor activity and feeding was used to evaluate the integrity of the circadian system (24). As expected, WT rats kept in the standard LD cycle show robust 24-h behavioral rhythms (Fig. 1*A* and *B*). In addition, rats also display robust circadian rhythms in glycemia (peak: 2200 h, trough: 200 h, $P < 0.05$; Fig. 1*C*) and C-peptide secretion (peak: 2200 h, trough: 0600 h, $P < 0.05$; Fig. 1*D*). To assess islet clock gene expression in vivo, we performed laser microdissection of islets from pancreatic tissue sections collected during the 24-h LD cycle. Key circadian clock transcriptional activator *Bmal-1* (peak: 0600 h, $P < 0.05$) and negative feedback regulator *Per-1* (peak: 1800 h, $P < 0.05$) showed robust antiphase expression consistent with the proposed model of the mammalian circadian clockwork (Fig. 1*E*). Furthermore, immunofluorescence confirmed diurnal oscillations in clock protein

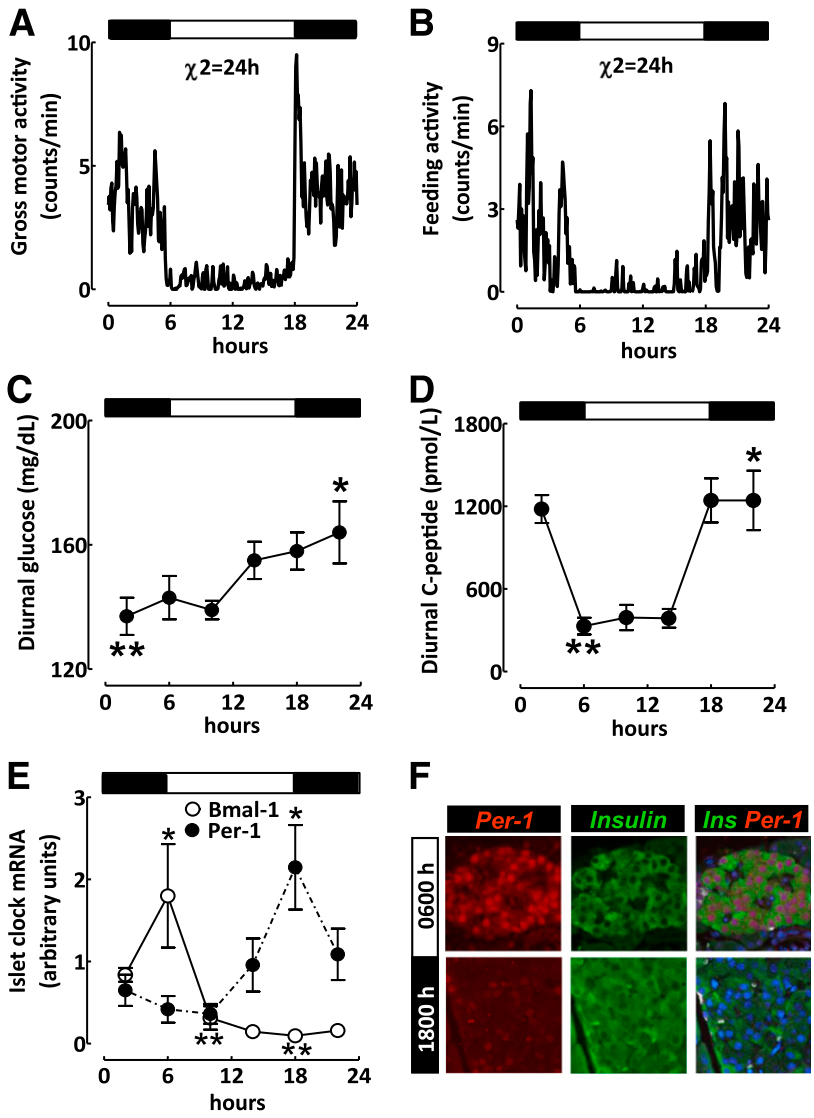

FIG. 1. Robust behavioral, metabolic, and islet molecular circadian rhythms in rats maintained under standard LD cycle conditions. Representative mean daily measurements of diurnal gross motor (*A*) and feeding activity (*B*) in rats exposed to typical light regimen (12:12 h, LD). Note rats exhibit robust diurnal 24-h behavioral rhythms. The black and white bars reflect the dark and light phase of the daily cycle, and χ^2 denotes the diurnal oscillation period. Diurnal profiles in plasma glucose (*C*) and C-peptide secretion (*D*) measured in rats at 4-h intervals (n = 4–5 rats per time point) across the 24-h day under typical LD cycle. *E*: Diurnal transcriptional profiles in BMAL-1 (○) and Per-1 (●) mRNA obtained from laser-microdissected islets from rats at 4-h intervals (n = 4–5 per time point) across the 24-h day under typical LD cycle. Note distinct antiphase relationship among Bmal-1 and Per-1 transcripts. *F*: Examples of pancreatic islets stained by immunofluorescence for insulin (green), Per-1 (red), and nuclei (blue) in rats euthanized during the "lights on" (0600-h) or "lights off" (1800-h) period. Data are expressed as mean ± SEM. *$P < 0.05$ denotes statistical significance for peak value related to 24-h LD cycle. **$P < 0.05$ denotes statistical significance for trough value related to 24-h LD cycle.

expression localized to β-cells (Fig. 1*F* and Supplementary Fig. 1).

Longitudinal assessment of rat islet circadian clock using islets isolated from *Per-1*:LUC rats. Tracking of cell bioluminescence with a clock gene luciferase fusion construct was used for assessment of islet circadian oscillators ex vivo (25). Islets cultured in standard islet media (11 mmol/L glucose) displayed sustained circadian rhythms in *Per-1* bioluminescence, with a robust amplitude, oscillatory period, and the phase of circadian oscillations reflected the temporal profile of in vivo *Per-1* mRNA expression (peak: 20.2 ± 0.6 h; Fig. 2*A–D* and Supplementary Fig. 2). Islet circadian clocks also demonstrated glucose sensitivity (Fig. 2*A–D*). Specifically, islets cultured at low glucose (2 or 5 mmol/L) showed a reduction in the amplitude (3.7-fold, $P < 0.05$ vs. 11 mmol/L), lengthening of the oscillatory period (27.5 ± 0.5 vs. 22.3 ± 0.1 h, $P < 0.01$ vs. 11 mmol/L), and altered phase (peak: 7 ± 0.9 vs. 20.2 ± 0.6 h, $P < 0.05$ vs. 11 mmol/L) of *Per-1* bioluminescence oscillations (Fig. 2*A–D*). Exposure to hyperglycemic conditions (25 mmol/L) did not alter the amplitude, period, or the phase of the islet circadian clock (Fig. 2).

The amplitude of *Per-1* bioluminescence in islets gradually dampened over time, as would be expected in the absence of the input from the SCN (21). However, activation of cAMP-response element binding protein (a mediator of circadian clock entrainment) with Forskolin (10 μmol/L) restarted *Per*-driven bioluminescence oscillations, confirming that dampening was not due to tissue attrition (Supplementary Fig. 3). Moreover, circadian oscillations in *Per-1* bioluminescence were also detected

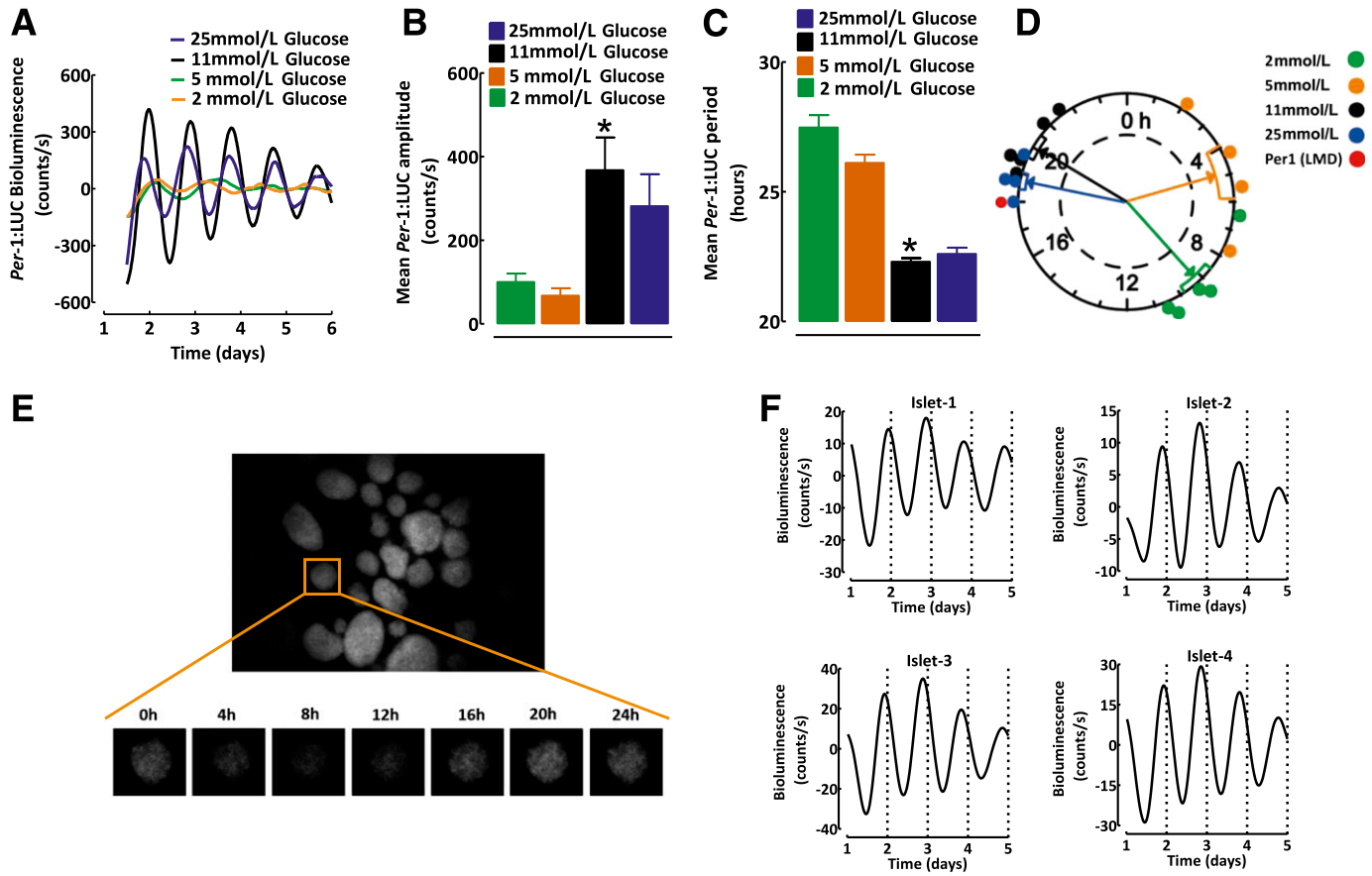

FIG. 2. Continuous longitudinal monitoring of the islet circadian clock using *Per-1*:LUC rats. *A*: Representative examples of Per-driven diurnal bioluminescence rhythms in batches of 50 islets isolated from *Per-1*:LUC rats cultured in standard islet media for 7 days at 2 (orange), 5 (green), 11 (black), or 25 mmol/L (blue) glucose concentrations. Corresponding mean amplitude (*B*) and period (*C*) of Per-driven diurnal bioluminescence rhythms in islets isolated from *Per-1*:LUC rats cultured for 7 days at 2, 5, 11, or 25 mmol/L glucose concentrations (n = 4–5 per condition). *D*: Rayleigh vector plot with individual time points representing the timing of the peak *Per*-1:LUC expression relative to the 24-h day LD cycle (n = 4–5 independent experiments) in batches of 50 islets cultured at 2, 5, 11, and 25 mmol/L glucose concentrations. Rayleigh vector plots were used to assess the significance of phase clustering of peak phases of Per-1 expression in relation to circadian time. Each filled circle indicates the phase (time) of peak *Per*-1:LUC bioluminescence in individual cultures of isolated islets under various glucose levels. The direction of an arrow indicates the mean phase vector and its length indicates the significance relative to $P < 0.05$, with the significance threshold indicated by the inner broken circle. The rectangular boxes surrounding arrowheads show variance (SE) of phase between individual experiments. Note that the peak Per-1 mRNA expression obtained through laser microdissection of islets (described in Fig. 1) is shown (red circle) to reflect the phase of Per-1 diurnal oscillations in vivo. *E*: Whole-field image (original magnification ×10) of islets isolated from *Per-1*:LUC transgenic rats under standard LD condition taken by intensified charge-coupled device camera. An individual islet image was collected over 24 h from the islet in the orange square in the figure. *F*: Examples of corresponding Per-driven bioluminescence rhythms obtained from four individual islets shown in *E* isolated from *Per-1*:LUC rats under the standard LD cycle cultured in 11 mmol/L glucose. Note the robust in-phase oscillations among individual islets. Data are expressed as mean ± SEM. *$P < 0.05$ denotes statistical significance for 11 vs. 2 and 5 mmol/L glucose. LMD, laser microdissection.

from single islets that displayed robust in-phase oscillations (Fig. 2*E* and *F*).

Islet circadian clock is entrained by changes in the LD cycle. We next investigated whether changes in the LD cycle can entrain and thus set the phase of islet clock transcriptional oscillations. To accomplish this, we inverted the phase of the LD cycle in *Per-1*:LUC transgenic rats by 12 h from LD (lights on at 0600 h, lights off at 1800 h) to DL (lights on at 1800 h, lights off 0600 h; Fig. 3*A*). Reversal of the LD cycle to the new DL cycle resulted in 12-h reversal of behavioral activity, confirming the success of the SCN photoentrainment (Fig. 3*A* and *B*). Subsequently, transition of the photoperiod from LD to DL resulted in near 12-h phase reversal of islet *Per-1*:LUC bioluminescence signal (peak: 22.2 ± 0.1 vs. 13.5 ± 0.6 h for LD vs. DL, $P < 0.05$; Fig. 3*C* and *D*) with no change in oscillatory period or the amplitude.

Circadian disruption due to LL disrupts islet circadian clock. Increased exposure to LL disrupts circadian rhythms and augments susceptibility to T2DM in humans (26,27). Thus, we next set out to address whether chronic exposure to LL disrupts islet circadian clock function. We exposed 2-month-old *Per-1*:LUC rats to 10 weeks of the normal LD cycle or LL regimen. As expected, exposure to LL in rats resulted in behavioral arrhythmicity (Fig. 4*A* and *B*) and abolished circadian rhythms in calculated indices of insulin sensitivity and β-cell function derived from HOMA, $HOMA_{IR}$, and $HOMA_{\beta}$ (Fig. 4*C* and *D*). Importantly, exposure to LL led to the dampening in the amplitude of *Per1*-driven luciferase oscillations in isolated islets but did not affect the oscillatory period of *Per1*-driven oscillations (Fig. 4*E* and *F*). We further confirmed this observation at the single islet level by using intensified charge-coupled device camera recordings (Fig. 5). Whereas individual islets isolated from LD rats showed well-defined, in-phase, high-amplitude circadian cycles of *Per1*-driven luciferase expression, LL rats exhibited dampened amplitude (80%; LD vs. LL, $P < 0.05$; Fig. 5*C*) of circadian

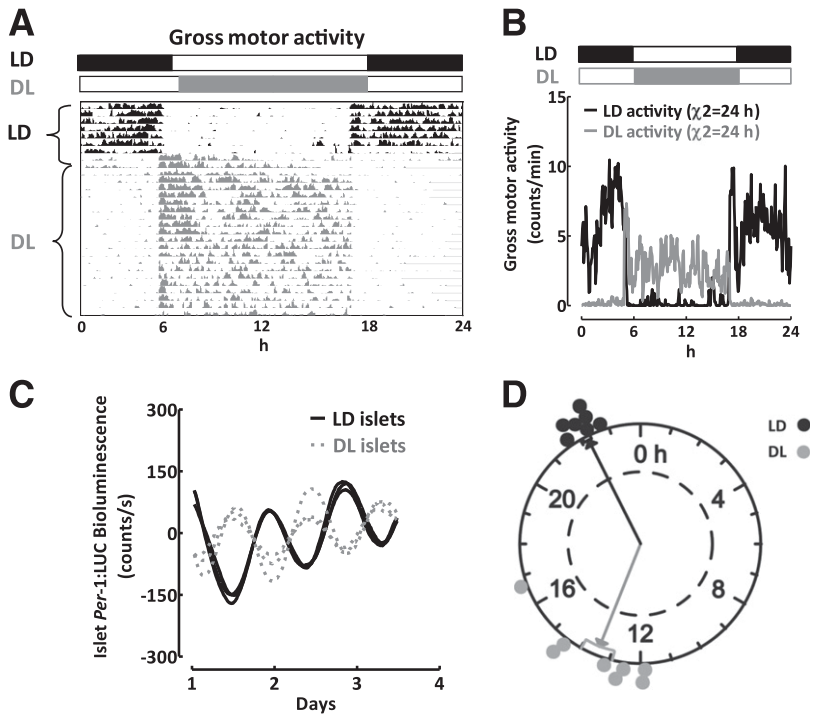

FIG. 3. Photoperiod entrains the phase of the islet circadian clock. *A*: An actogram of gross motor activity recordings in a representative *Per-1*:LUC rat exposed to 7 days of standard LD cycle (lights on at 0600 h, lights off at 1800 h; black), followed by DL, a 12-h reversal of the light cycle (lights on at 1800 h, lights off at 0600 h; gray) for the next 30 days. *B*: Mean diurnal measurements of gross motor activity obtained at 3-min intervals in rats exposed to standard LD (black lines) or DL (gray lines). The black and white bars reflect the dark and light phase of the daily cycle, and χ^2 denotes diurnal oscillation period in activity. *C*: Representative examples of diurnal bioluminescence rhythms in three independent batches of 50 islets isolated from *Per-1*:LUC rats exposed to 30 days of LD (black lines) vs. DL (gray lines) cycle. Note the antiphase dynamics of the *Per*-1:LUC signal. *D*: Rayleigh plot with individual time points representing the timing of the peak *Per*-1:LUC expression relative to the 24-h day in $n = 7–8$ independent batches of 50 islets isolated from *Per-1*:LUC rats exposed to 30 days of LD (black) vs. DL (gray) cycle. Rayleigh vector plots were used to assess the significance of phase clustering of peak phases of Per-1 expression in relation to circadian time. Each filled circle indicates the phase (time) of peak *Per*-1:LUC bioluminescence in individual cultures of isolated islets from rats exposed to LD (black) or DL (gray) cycle. The direction of an arrow indicates the mean phase vector, and its length indicates the significance relative to $P < 0.05$, with significance threshold indicated by the inner broken circle. The rectangular boxes surrounding the arrowheads show variance (SE) of phase between individual experiments.

oscillations. Furthermore, *Per-1* bioluminescence recorded from LL islets showed impaired phase and the synchrony of *Per*-driven luciferase oscillations among individual islets (peak: 22.5 ± 0.1 vs. 17.6 ± 0.5 h for LD vs. LL, $P < 0.05$; Fig. 5*E*). Interestingly, LL-treated islets still maintained a robust period of clock oscillations (Fig. 5*D*).

Effects of circadian disruption due to LL on β-cell function in vitro. To assess whether prolonged exposure to LL has deleterious effects on β-cell secretory capacity, we exposed 2-month-old rats to 10 weeks of LD or LL cycle, confirmed disruption of circadian rhythms in LL via activity monitoring, and assessed insulin secretion in vitro in islets by static incubation and islet perifusion (Fig. 6). In islets isolated from LD animals, dose-dependent glucose stimulation induced by 8, 12, and 16 mmol/L glucose led to a robust increase in insulin release of approximately three-, four-, and fivefold versus 4 mmol/L, respectively ($P < 0.05$ at each glucose concentration; Fig. 6*A* and *B*). In contrast, LL islets showed blunted glucose-responsiveness, with only 16 mmol/L glucose eliciting a significant increase in insulin release from baseline (Fig. 6*A* and *B*). Insulin response to nonglucose secretory stimuli, such as exendin-4 and tolbutamide, remained intact in LL animals, suggesting a primary defect in glucose metabolism and/or coupling to oxidative phosphorylation (Fig. 6*C*). To elucidate the mechanism underlying diminished glucose-stimulated insulin release, we performed islet perifusions to assess the pulsatile mode of insulin secretion (Fig. 6*D–I*). LL-treated islets demonstrated blunted glucose-stimulated insulin secretion (~40% vs. LD, $P < 0.05$), which was due to an ~40% deficit in insulin secretory pulse mass, with no alteration in the frequency of pulsatile insulin release (Fig. 6*D–I*).

DISCUSSION

The mammalian circadian system is organized as a multilevel oscillator network. The main SCN oscillator is synchronized to the LD cycle through specialized retinal ganglion cells, with light serving as the principal entrainment stimuli (28). The SCN, in turn, plays a central role in synchronizing the rhythms of the peripheral circadian clocks to the 24-h LD cycle (29). This multilevel circadian oscillator system undoubtedly provides an evolutionary advantage for human health. However, because the circadian system is sensitive to changes in the LD cycle, disruption of circadian rhythms as a result of shift work, sleep loss, exposure to LL, and other factors has been associated with deleterious health consequences (30,31).

Specifically, circadian disruption is associated with development of T2DM, a relationship partly attributed to islet failure (5–8,10,18,19). This implicates disturbances in the islet circadian clock as a potential molecular mechanism underlying the association between circadian disruption,

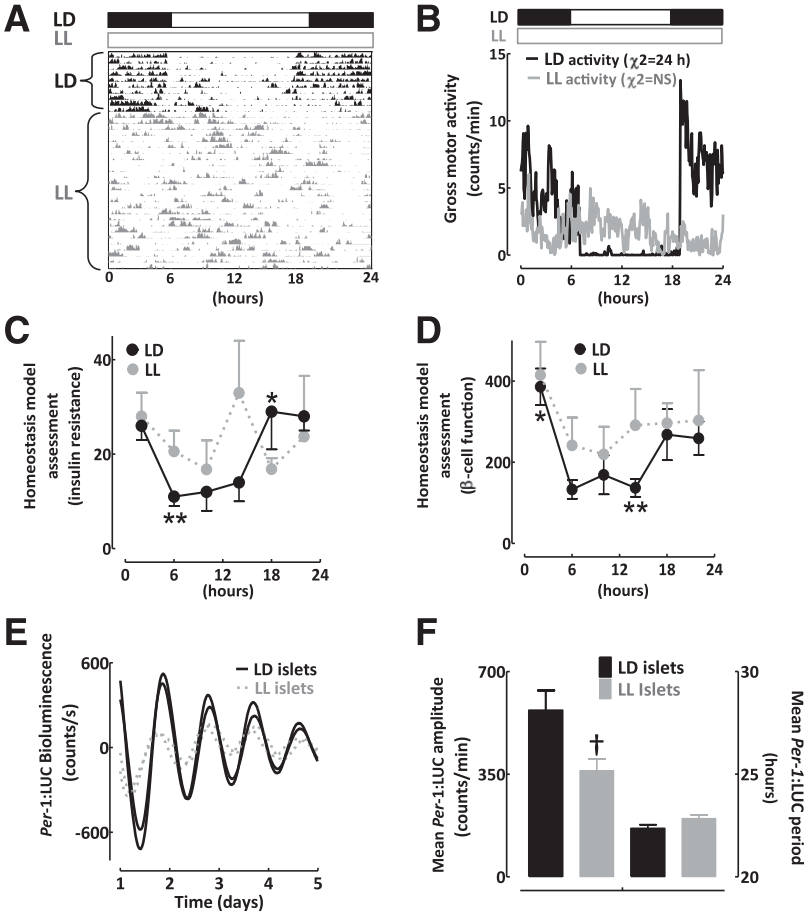

FIG. 4. Exposure to LL disrupts behavioral, metabolic, and islet molecular circadian rhythms in rats. *A*: An actogram recording of gross motor activity in a representative *Per-1*:LUC rat exposed to 7 days of standard LD (black) cycle, followed by exposure to LL (gray) cycle for the next 10 weeks (4 weeks of LL is shown). *B*: Mean diurnal measurements of gross motor activity in rats exposed to 10 weeks of standard LD (black lines) or LL (gray lines) cycle. The black and white bars reflect the dark and light phase of the daily cycle, and χ^2 denotes diurnal oscillation period. Note complete behavioral arrhythmicity in LL rats. Diurnal profiles in the calculated indices of insulin sensitivity (*C*) and β-cell function (*D*) derived from HOMA, $HOMA_{IR}$, and $HOMA_{\beta}$ (see RESEARCH DESIGN AND METHODS for calculations) in rats obtained at 4-h intervals (n = 4–5 per time point) across the 24-h day under standard LD (black circles) and disrupted LL (gray circles) cycles. *E*: Representative examples of diurnal bioluminescence rhythms in two independent batches of 50 islets isolated from *Per-1*:LUC rats exposed to 10 weeks of LD (black lines) vs. LL (gray lines) cycle. *F*: Mean amplitude and period of diurnal bioluminescence rhythms in batches of 50 islets isolated from *Per-1*:LUC rats exposed to 10 weeks of LD (open bars) vs. LL (gray bars) cycle (n = 4–5 per condition). Data are expressed as mean ± SEM. *$P < 0.05$ denotes statistical significance for peak value related to 24-h LD cycle. **$P < 0.05$ denotes statistical significance for trough value related to 24-h LD cycle. †$P < 0.05$ denotes statistical significance for LD vs. LL.

T2DM, and islet failure. Thus, in the current study, we sought to elucidate effects of the environmental conditions associated with circadian rhythm disruption common to modern life on the islet circadian clock and function. To address this, we first validated the use of *Per-1*:LUC rats for assessment of islet clock function ex vivo. Secondly, we established that changes in the LD cycles in vivo entrain the phase of islet clock transcriptional oscillations. Thirdly, we demonstrated that exposure to LL disrupts islet circadian clock function through impairment in the amplitude, phase, and interislet synchrony of clock transcriptional oscillations. Finally, we also report that islets isolated from rats exposed to LL exhibit diminished glucose-stimulated insulin secretion attributed to the deficit in insulin secretory pulse mass.

Evidence supports a role for the β-cell circadian clock in regulation of insulin secretion and β-cell survival. Circadian rhythms in glucose tolerance and β-cell secretory capacity have been observed under fasting, glucose-infusion, and meal conditions (15,32,33). Importantly, lesioning of the SCN in rats or exposure to LL abolishes circadian rhythms in glucose tolerance and insulin release and impairs β-cell function (16). This suggests that the central clock regulates diurnal insulin secretion, plausibly through influencing β-cell circadian clock function. In support of this hypothesis, pancreas-specific CLOCK and BMAL-1 mutant mice demonstrate a loss of diurnal rhythms in glucose tolerance and insulin secretion and exhibit diminished β-cell function (10,18). Furthermore, pancreas-specific clock mutants also show impaired expression of genes regulating islet growth, survival, and proliferation, emphasizing that the islet circadian clock may also be significant in the regulation of β-cell survival (10). Indeed, cellular response to oxidative and endoplasmic reticulum stress is under transcriptional control of the circadian clock (34). This is significant because both of these features contribute to islet failure in diabetes (35,36). Interestingly, circadian disruption due to prolonged exposure to LL in rats increases β-cell vulnerability to apoptosis associated with overexpression of human islet amyloid polypeptide, a known inducer of β-cell endoplasmic reticulum stress (8).

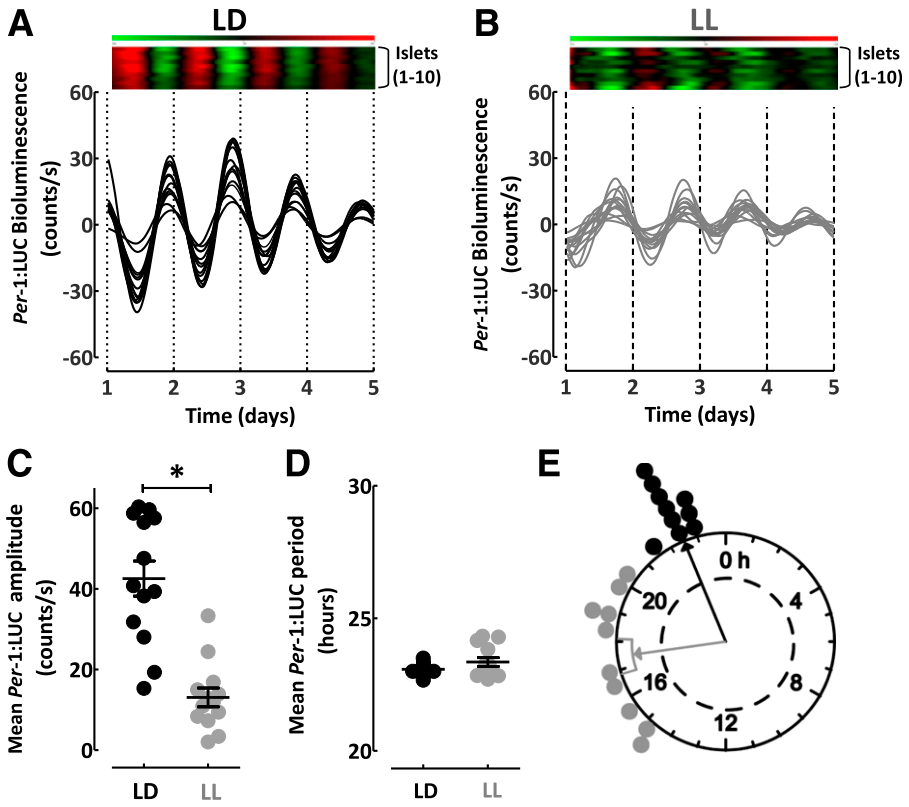

FIG. 5. Exposure to LL disrupts the amplitude, phase, and coordination of molecular circadian rhythms in individual pancreatic islets. Representative examples of Per-driven diurnal bioluminescence rhythms imaged by intensified charge-coupled device camera at the level of individual islets (n = 13) from *Per-1*:LUC rats exposed to 10 weeks of LD cycle (black lines) (*A*) or aberrant LL cycle (gray lines) (*B*). Each black or gray line represents Per-driven bioluminescence signal from an individual islet. Raster plots shown on top of the each graph represent corresponding diurnal *Per*-1:LUC expression in 10 individual islets across the 5-day recording period, with green color representing the peak and red color the trough expression. Note the apparent loss of the amplitude and synchrony in *Per*-1:LUC expression among individual islets in LL rats. Mean amplitude (*C*) and period (*D*) of *Per*-1:LUC oscillations in individual islets from rats exposed to 10 weeks of LD (black) vs. LL (gray) cycle. *E*: Rayleigh plot with each filled circle indicating the phase (time) of peak *Per*-1:LUC bioluminescence in an individual islet from rats exposed to 10 weeks of LD (black) or LL (gray) cycle. The direction of an arrow indicates the mean phase vector, and its length indicates the significance relative to $P < 0.05$, with significance threshold indicated by the inner broken circle. The rectangular boxes surrounding the arrowheads show variance (SE) of phase between individual LD or LL islets. *$P < 0.05$ denotes statistical significance for LD vs. LL.

One of the key observations in our study is that exposure to LL leads to dampening, alterations in the phase, and desynchrony of islet clock transcriptional rhythms. This can be attributed to disruption or altered function of the SCN clock resulting in impaired entrainment of circadian oscillators in islets. Indeed, prolonged exposure to LL (of similar duration and light intensity used in our study) leads to desynchronization of circadian oscillators in the SCN, resulting in the loss of behavioral and endocrine rhythms (37). Similar abolishment of circadian behavioral and endocrine rhythms is observed after SCN lesioning in rodents, which can be partially restored upon SCN transplantation (38,39). Importantly, SCN lesions are associated with damping of the amplitude of circadian clock oscillations in peripheral tissues (e.g., liver and kidney) (40,41), albeit with some studies only noting alterations in the phase of transcriptional oscillations (42). Consistent with our findings, these studies suggest that surgical or light-induced disruption of the SCN circadian clock can result in impaired cyclical expression, dampened amplitude, and altered phase of circadian clock transcriptional oscillations in peripheral tissue. Moreover, our work also shows that in some parallels to the results obtained by lesioning the SCN (37), exposure to LL results in impaired coupling among individual circadian oscillators in pancreatic islets. The functional significance of uncoupling individual circadian oscillators in islets is unknown; however, synchronization of individual neuronal clocks in the SCN is essential for proper clock function (43).

Mechanisms have been proposed to mediate entrainment of peripheral oscillators by the SCN (29). However, which mechanism(s) regulate entrainment of islet circadian clocks are currently unknown. The SCN has been shown to modulate peripheral clock expression through the autonomic nervous system (44). Pancreatic islets receive extensive innervation by the autonomic nervous system, and the SCN has been shown to innervate the pancreas via the parasympathetic neuronal pathway (45). The SCN also has been shown to modulate entrainment of peripheral clocks through circadian regulation of hormonal release (e.g., corticosterone and melatonin) (29). Recent work on the role of melatonin receptor signaling in the regulation of islet failure in T2DM suggests that the significance of diurnal melatonin secretion for entrainment of islet clocks merits further investigation (46). In addition, the SCN also controls diurnal feeding, the timing of which has been shown to entrain the phase and the amplitude of peripheral clocks, particularly in organs, such the liver and the pancreas, responsive to nutrient availability (20,47). In our study, exposure to LL was associated with the loss of circadian rhythms in hormonal release (melatonin and corticosterone) and in feeding behavior. However, further

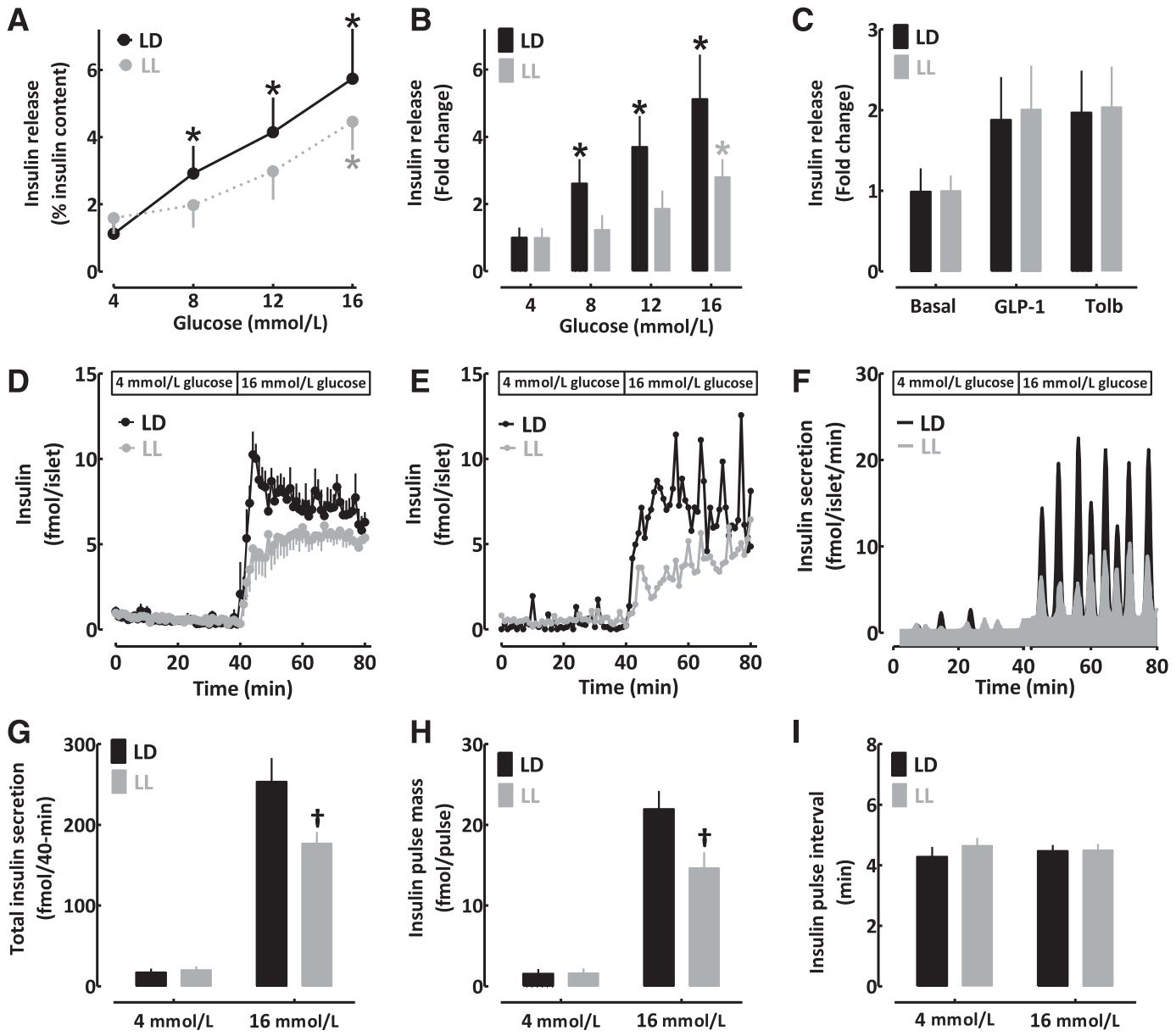

FIG. 6. Effects of circadian disruption due to LL on glucose-stimulated insulin secretion in isolated islets. Glucose-stimulated insulin release expressed as percentage of insulin content (*A*) or fold change above basal (*B*) in isolated islets from rats exposed to 10 weeks of standard LD (black lines/bars) or LL (gray lines/bars) cycle (n = 7 per condition). *C*: Insulin release after stimulation with nonglucose secretory stimuli GLP-1 (10 nmol/L exendin-4) and sulfonylurea (250 μmol/L tolbutamide [Tolb]) in isolated islets from rats exposed to 10 weeks of standard LD (black bars) or LL (gray bars) cycle (n = 5 per condition). *D*: Mean insulin concentration profiles during islet perifusion at 4 (0–40 min) and 16 mmol/L glucose (40–80 min) in isolated islets from rats exposed to 10 weeks of standard LD (black lines) or LL (gray lines) cycle (n = 5 per condition). Representative islet perifusion insulin concentration (*E*) and derived insulin secretion (*F*) rates during islet perifusion at 4 (0–40 min) and 16 mmol/L glucose (40–80 min) in isolated islets from a rat exposed to 10 weeks of standard LD (black lines) or LL (gray lines) cycle. Mean insulin secretion (*G*), insulin secretory pulse mass (*H*), and insulin pulse interval (*I*) during islet perifusion at 4 (0–40 min) and 16 mmol/L glucose (40–80 min) in isolated islets from rats exposed to 10 weeks of standard LD (black bars) or LL (gray bars) cycle (n = 5 per condition). Data are expressed as mean ± SEM. *P < 0.05 denotes statistical significance vs. 4 mmol/L glucose condition. †P < 0.05 denotes statistical significance vs. LD.

work is needed to delineate exact mechanisms regulating entrainment of clocks in islets.

This report also examined effects of prolonged exposure to LL on β-cell function in isolated islets. Our observation that prior exposure to LL results in diminished β-cell function is consistent with findings in humans that report induction of glucose intolerance and diminished insulin response to glucose after circadian misalignment (7,17). Our data are also consistent with findings reported in rodents with genetic mutations in the core components of the circadian clock genes, which also demonstrate diminished β-cell glucose-responsiveness hypothesized to be associated with defective insulin exocytosis and/or mitochondrial uncoupling leading to diminished glucose-induced mitochondrial potential and ATP production (10,48).

In conclusion, we established and validated methods for continuous longitudinal monitoring of islet circadian clocks ex vivo using *Per-1*:LUC rats. Using this methodology, we demonstrated that islet clock transcriptional oscillations are entrained by changes in the LD cycle and found that disruption of circadian rhythms due to exposure to LL disturbs islet circadian clock and β-cell function

in vitro. Our data suggest that impaired islet clock function caused by circadian system disruption may be responsible for altered islet function and survival and consequent predisposition to T2DM.

ACKNOWLEDGMENTS

This work was supported by grants from the National Institutes of Health (K01DK089003) and the Larry L. Hillblom Foundation to A.V.M. and the Esther B. O'Keefe Foundation to A.V.M. and C.S.C.

No potential conflicts of interest relevant to this article were reported.

J.Q. assisted with design of the studies, performed studies, and assisted with interpretation of the studies and preparation of the manuscript. G.D.B. and C.S.C. assisted with study design and interpretation and reviewed and edited the manuscript. A.V.M. contributed to study design and interpretation and wrote the manuscript. A.V.M is the guarantor of this work and, as such, had full access to all of the data in the study and takes responsibility for the integrity of the data and the accuracy of the data analysis.

The authors thank the members of the laboratories of Dr. Joseph Bass (Northwestern University) and Dr. Christopher Colwell (UCLA) for excellent suggestions in developing conditions for islet bioluminescence recordings. The authors are grateful to Bonnie Yeh (UCLA) and Kevin Hsu (UCLA) for excellent technical support and animal care. The authors also thank Dr. Peter C. Butler (UCLA) for helpful discussions and insightful comments.

REFERENCES

1. Butler AE, Janson J, Bonner-Weir S, Ritzel R, Rizza RA, Butler PC. Beta-cell deficit and increased beta-cell apoptosis in humans with type 2 diabetes. Diabetes 2003;52:102–110
2. Seltzer HS, Allen EW, Herron AL Jr, Brennan MT. Insulin secretion in response to glycemic stimulus: relation of delayed initial release to carbohydrate intolerance in mild diabetes mellitus. J Clin Invest 1967;46:323–335
3. Cornelis MC, Hu FB. Gene-environment interactions in the development of type 2 diabetes: recent progress and continuing challenges. Annu Rev Nutr 2012;32:245–259
4. Nilsson PM, Rööst M, Engström G, Hedblad B, Berglund G. Incidence of diabetes in middle-aged men is related to sleep disturbances. Diabetes Care 2004;27:2464–2469
5. Pan A, Schernhammer ES, Sun Q, Hu FB. Rotating night shift work and risk of type 2 diabetes: two prospective cohort studies in women. PLoS Med 2011;8:e1001141
6. Spiegel K, Leproult R, Van Cauter E. Impact of sleep debt on metabolic and endocrine function. Lancet 1999;354:1435–1439
7. Buxton OM, Cain SW, O'Connor SP, et al. Adverse metabolic consequences in humans of prolonged sleep restriction combined with circadian disruption. Sci Transl Med 2012;4:129ra143
8. Gale JE, Cox HI, Qian J, Block GD, Colwell CS, Matveyenko AV. Disruption of circadian rhythms accelerates development of diabetes through pancreatic beta-cell loss and dysfunction. J Biol Rhythms 2011;26:423–433
9. Reppert SM, Weaver DR. Coordination of circadian timing in mammals. Nature 2002;418:935–941
10. Marcheva B, Ramsey KM, Buhr ED, et al. Disruption of the clock components CLOCK and BMAL1 leads to hypoinsulinaemia and diabetes. Nature 2010;466:627–631
11. Buijs RM, Kalsbeek A. Hypothalamic integration of central and peripheral clocks. Nat Rev Neurosci 2001;2:521–526
12. Gekakis N, Staknis D, Nguyen HB, et al. Role of the CLOCK protein in the mammalian circadian mechanism. Science 1998;280:1564–1569
13. Lee C, Etchegaray JP, Cagampang FR, Loudon AS, Reppert SM. Post-translational mechanisms regulate the mammalian circadian clock. Cell 2001;107:855–867
14. Bass J, Takahashi JS. Circadian integration of metabolism and energetics. Science 2010;330:1349–1354
15. Boden G, Ruiz J, Urbain JL, Chen X. Evidence for a circadian rhythm of insulin secretion. Am J Physiol 1996;271:E246–E252
16. la Fleur SE, Kalsbeek A, Wortel J, Fekkes ML, Buijs RM. A daily rhythm in glucose tolerance: a role for the suprachiasmatic nucleus. Diabetes 2001;50:1237–1243
17. Qin LQ, Li J, Wang Y, Wang J, Xu JY, Kaneko T. The effects of nocturnal life on endocrine circadian patterns in healthy adults. Life Sci 2003;73:2467–2475
18. Sadacca LA, Lamia KA, deLemos AS, Blum B, Weitz CJ. An intrinsic circadian clock of the pancreas is required for normal insulin release and glucose homeostasis in mice. Diabetologia 2011;54:120–124
19. Vieira E, Marroquí L, Batista TM, et al. The clock gene Rev-erbα regulates pancreatic β-cell function: modulation by leptin and high-fat diet. Endocrinology 2012;153:592–601
20. Stokkan KA, Yamazaki S, Tei H, Sakaki Y, Menaker M. Entrainment of the circadian clock in the liver by feeding. Science 2001;291:490–493
21. Yamazaki S, Numano R, Abe M, et al. Resetting central and peripheral circadian oscillators in transgenic rats. Science 2000;288:682–685
22. Song SH, Kjems L, Ritzel R, et al. Pulsatile insulin secretion by human pancreatic islets. J Clin Endocrinol Metab 2002;87:213–221
23. Matthews DR, Hosker JP, Rudenski AS, Naylor BA, Treacher DF, Turner RC. Homeostasis model assessment: insulin resistance and beta-cell function from fasting plasma glucose and insulin concentrations in man. Diabetologia 1985;28:412–419
24. Stephan FK, Zucker I. Circadian rhythms in drinking behavior and locomotor activity of rats are eliminated by hypothalamic lesions. Proc Natl Acad Sci U S A 1972;69:1583–1586
25. Welsh DK, Imaizumi T, Kay SA. Real-time reporting of circadian-regulated gene expression by luciferase imaging in plants and mammalian cells. Methods Enzymol 2005;393:269–288
26. Pauley SM. Lighting for the human circadian clock: recent research indicates that lighting has become a public health issue. Med Hypotheses 2004;63:588–596
27. Kivimäki M, Batty GD, Hublin C. Shift work as a risk factor for future type 2 diabetes: evidence, mechanisms, implications, and future research directions. PLoS Med 2011;8:e1001138
28. Hattar S, Liao HW, Takao M, Berson DM, Yau KW. Melanopsin-containing retinal ganglion cells: architecture, projections, and intrinsic photosensitivity. Science 2002;295:1065–1070
29. Saini C, Suter DM, Liani A, Gos P, Schibler U. The mammalian circadian timing system: synchronization of peripheral clocks. Cold Spring Harb Symp Quant Biol 2011;76:39–47
30. Reddy AB, O'Neill JS. Healthy clocks, healthy body, healthy mind. Trends Cell Biol 2010;20:36–44
31. Takahashi JS, Hong HK, Ko CH, McDearmon EL. The genetics of mammalian circadian order and disorder: implications for physiology and disease. Nat Rev Genet 2008;9:764–775
32. Freinkel N, Mager M, Vinnick L. Cyclicity in the interrelationships between plasma insulin and glucose during starvation in normal young men. J Lab Clin Med 1968;71:171–178
33. Saad A, Dalla Man C, Nandy DK, et al. Diurnal pattern to insulin secretion and insulin action in healthy individuals. Diabetes 2012;61:2691–2700
34. Kondratov RV, Kondratova AA, Gorbacheva VY, Vykhovanets OV, Antoch MP. Early aging and age-related pathologies in mice deficient in BMAL1, the core componentof the circadian clock. Genes Dev 2006;20:1868–1873
35. Huang CJ, Lin CY, Haataja L, et al. High expression rates of human islet amyloid polypeptide induce endoplasmic reticulum stress mediated beta-cell apoptosis, a characteristic of humans with type 2 but not type 1 diabetes. Diabetes 2007;56:2016–2027
36. Sakuraba H, Mizukami H, Yagihashi N, Wada R, Hanyu C, Yagihashi S. Reduced beta-cell mass and expression of oxidative stress-related DNA damage in the islet of Japanese Type II diabetic patients. Diabetologia 2002;45:85–96
37. Ohta H, Yamazaki S, McMahon DG. Constant light desynchronizes mammalian clock neurons. Nat Neurosci 2005;8:267–269
38. Turek FW. Circadian neural rhythms in mammals. Annu Rev Physiol 1985;47:49–64
39. Ralph MR, Foster RG, Davis FC, Menaker M. Transplanted suprachiasmatic nucleus determines circadian period. Science 1990;247:975–978
40. Akhtar RA, Reddy AB, Maywood ES, et al. Circadian cycling of the mouse liver transcriptome, as revealed by cDNA microarray, is driven by the suprachiasmatic nucleus. Curr Biol 2002;12:540–550
41. Tahara Y, Kuroda H, Saito K, et al. In vivo monitoring of peripheral circadian clocks in the mouse. Curr Biol 2012;22:1029–1034
42. Yoo SH, Yamazaki S, Lowrey PL, et al. PERIOD2:LUCIFERASE real-time reporting of circadian dynamics reveals persistent circadian oscillations

in mouse peripheral tissues. Proc Natl Acad Sci U S A 2004;101:5339–5346
43. Aton SJ, Colwell CS, Harmar AJ, Waschek J, Herzog ED. Vasoactive intestinal polypeptide mediates circadian rhythmicity and synchrony in mammalian clock neurons. Nat Neurosci 2005;8:476–483
44. Okamura H. Suprachiasmatic nucleus clock time in the mammalian circadian system. Cold Spring Harb Symp Quant Biol 2007;72:551–556
45. Ueyama T, Krout KE, Nguyen XV, et al. Suprachiasmatic nucleus: a central autonomic clock. Nat Neurosci 1999;2:1051–1053
46. Mulder H, Nagorny CL, Lyssenko V, Groop L. Melatonin receptors in pancreatic islets: good morning to a novel type 2 diabetes gene. Diabetologia 2009;52:1240–1249
47. Damiola F, Le Minh N, Preitner N, Kornmann B, Fleury-Olela F, Schibler U. Restricted feeding uncouples circadian oscillators in peripheral tissues from the central pacemaker in the suprachiasmatic nucleus. Genes Dev 2000;14:2950–2961
48. Lee J, Kim MS, Li R, et al. Loss of Bmal1 leads to uncoupling and impaired glucose-stimulated insulin secretion in β-cells. Islets 2011;3:381–388